DOES ELASTIC REBOUND THEORY APPLY TO SEISMIC FAULTS?

A. Ziv[1], A. Cochard[2] and J. Schmittbuhl[3,4]

[1] **Ben-Gurion University of the Negev, Beer-Sheva, Israel**

[2] **EES Dept, Ludwig-Maximilians-Universität, Munich, Germany**

[3] **Geology Lab., Ecole Normale Supérieure, Paris, France**

[4] **Institut de Physique du Globe, Strasbourg, France**

ABSTRACT

We examine the evolution of and the exchange between two forms of elastic energies stored in the quasi-dynamic fault model of *Ziv and Cochard* [1]. The first, E_{tect}, is due to the integrated slip deficit accumulated between the plate boundaries and the fault surface, and the second, E_{fault}, is the elastic energy stored as a result of differential slip along the fault surface. Time series of these energies show that large earthquakes occur during the descending portions of the E_{tect}-curve, and close to the maxima of the E_{fault}-curve. Interestingly, these results are not in agreement with the classical view of the elastic rebound theory (*Reid*, [2]). While the elastic rebound theory predicts that large earthquakes occur at the maxima of the E_{tect}-curve, in our model they occur at the maxima of the E_{fault}-curve. The latter, arising from the slip heterogeneity along the fault, is not at all accounted for in the elastic rebound theory, on which present earthquake prediction models rely.

1 INTRODUCTION

According to the elastic rebound theory (*Reid's*, [2]) the seismic cycle consists of two phases. The first is the interseismic stage, during which elastic strain accumulates slowly with time due to the relative motion of the adjacent plates. The second is a seismic phase, during which the elastic strain that is stored in the medium is released abruptly. While the interseismic stage may last many years, the duration of the seismic phase is a few seconds or tens of seconds. This concept implies that major earthquakes occur when the elastic strain reaches local maxima, and that the timing and/or the size of major earthquakes are predictable. Indeed, present earthquake prediction models and hazard assessment rely on this theory. Nearly a century since the elastic rebound theory had been postulated, it is constructive to re-examine its underlying assumptions and to test its applicability to seismic faults.

In this study we test the validity of the elastic rebound theory in the quasi-dynamic fault model of *Ziv and Cochard* [1], which is a 3-D discrete model that employs a rate-and-state friction. Clearly the results of such an exercise are model dependent, and stress histories consistent with the elastic rebound theory may be observed in some models. Such is the case with the spring-slider systems (e.g., *Schmittbuhl et al.*, [3]) and 2-D fault models (e.g., *Ben-Zion et al.*, [4]), where occasional system-size earthquakes break periodically or quasi-periodically. The situation that is studied here is different in that the occurrence of large earthquakes is non-periodic, and the largest events do not rupture the entire model. Moreover, the distribution of event sizes is close to a power-law, with Omori type of clustering prior to and following large earthquakes.

2 THE MODEL

We model a long, vertical, strike-slip fault that is embedded in an elastic half-space (Figure 1). Similar to *Rice* [5] we calculate quasi-dynamic slip in a region that extends down to N_{depth}. This part of the model is represented by a computational grid of square cells that is periodic along strike,

with repeating length of N_{length}. Below N_{depth} the fault slips steadily at the plate velocity, V_{plate}. In addition to being loaded by steady creep from below, the fault is subjected to an additional constant stressing rate due to displacement applied at V_{plate} rate on parallel planes located at distance W on either side of the fault plane. The horizontal and vertical dimensions of the computational grid are $N_{length} = 128$ cells and $N_{depth} = 64$ cells, respectively.

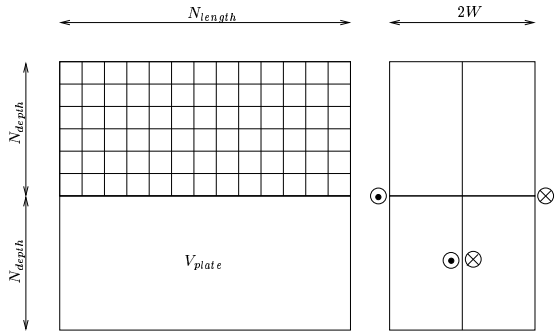

Figure 1: Schematic diagram showing strike-perpendicular (left) and strike-parallel (right) views of the model. The region over which motion is calculated is covered by $N_{length} \times N_{depth}$ computational cells. Displacement at rate V_{plate} is imposed on a co-planar substrate that extends below N_{depth} and down to $2N_{depth}$, and on fault-parallel planes located at distance W on either side of the fault plane.

Fault friction evolves with sliding speed, V, and fault state, θ, according to (*Dieterich*, [6]; *Ruina*, [7]):

$$\tau_i = \sigma_i(\mu_i^\star + A_i \ln \frac{V_i}{V_{plate}} + B_i \ln \frac{V_{plate}\theta_i}{D_c}), \tag{1}$$

where the subscript i denotes the index of the computational cell, σ is the effective normal stress, $\mu^\star$ is the friction coeffi cient when the fault slides steadily at the plate velocity V_{plate}, A and B are unitless parameters, and D_c is a characteristic distance for the evolution of the state from one steady state to another. In general, the three constitutive parameters A, B and D_c may be position-dependent. Here, however, A and B vary only with depth and D_c is fi xed. The state variable evolves with time, t, and slip history according to (*Ruina*, [8]):

$$\frac{d\theta_i}{dt} = 1 - \frac{V_i\theta_i}{D_c}. \tag{2}$$

At high slip speed, the second term on the right-hand side of (2) dominates, the state decreases exponentially with slip, and the cell weakens rapidly (*Dieterich*, [9]). At low speed, the state increases almost linearly with time, and the cell undergoes strengthening.
The evolution of the shear stress on cell i is written as a sum of four terms (*Ziv and Rubin* [11]):

$$\tau_i = \tau_i^0 + \frac{G}{W}(V_{plate}t - \delta_i) + \sum_j g_{ij}\delta_j - \frac{G}{2\beta}V_i. \tag{3}$$

The fi rst term, τ_i^0, is the initial stress. The second term represents the driving stresses imparted on the fault surface due to mismatch between the total displacement on the cell in question, δ_i, and the

cumulative tectonic slip imposed at rate V_{plate} at distance W on either side of the fault plane, with G being the shear modulus. The third term adds the elastic stress changes imposed on cell i due to slip on cells j, with g_{ij} being a 3-D elastic kernel. While cells labeled with i extends from the free surface down to N_{depth}, the summation over j extends from $2 \times N_{depth}$ below the free surface to $2 \times N_{depth}$ above the free surface. Finally, the forth term is an inertial term that embodies the quasi-dynamic approximation of *Rice* [5]. The factor $G/2\beta$, with β being the shear wave speed, is often referred to as the 'radiation damping'.
Stress balance yields (after derivation with respect to time):

$$\frac{dV_i}{dt} = \Big[\frac{G}{W}(V_{plate} - V_i) + \sum_j g_{ij}V_j - \frac{\sigma_i B_i}{\theta_i}\Big(1 - \frac{V_i\theta_i}{D_c}\Big)\Big] \times \Big(\frac{G}{2\beta} + \frac{\sigma_i A_i}{V_i}\Big)^{-1}. \qquad (4)$$

Notice that the evolution of V and θ is fully described by Equations (2) and (4). This set of differential equations is solved simultaneously at successive time steps using a Runge-Kutta algorithm.

3 ENERGY PARTITIONING

Following *Ziv and Schmittbuhl* [10], we introduce two elastic energy densities per unit area in the system immediately after an earthquake k: E^k_{tect} and E^k_{fault}. The first is due to the slip deficit accumulated between the plate boundaries and the fault surface, and is defined as:

$$E^k_{tect} = \frac{1}{N}\frac{G}{W}\sum_i [U_{tect}(t_k) - U_i(t_k)]^2, \qquad (5)$$

where G is the shear modulus, N is the number of computational cells, U_{tect} is the cumulative tectonic displacement increasing linearly with time, U_i is the cumulative slip on cell i increasing coseismically, and t_k is time immediately after event k. The second energy is the result of stress transfer due to slip on the fault, and is defined as:

$$E^k_{fault} = \frac{1}{2N}\sum_i \sum_j g_{ij}[U_i(t_k) - U_j(t_k)]^2 \qquad (6)$$

While E_{tect} is a measure of the mismatch between total slip of the plate boundary and cumulative slip on the fault, E_{fault} is a measure of the heterogeneity of the slip distribution.

4 RESULTS

Time series of these energies show that large earthquakes occur during the descending portions of the E_{tect}-curve, and close to the maxima of the E_{fault}-curve. On a E_{fault}-versus-E_{tect} plot, the seismic cycle has a roughly triangular shape with large earthquakes occurring at the top corner of the triangle, and the foreshocks and the aftershocks occupying the right side and left side, respectively. While both foreshocks and aftershocks dissipate tectonic energies, the cumulative effect of the foreshocks is to increase the fault disorder and the cumulative effect of the aftershocks is to reduce it.
Interestingly, these results are not in agreement with the classical view of the elastic rebound theory (*Reid*, [2]). While the elastic rebound theory predicts that large earthquakes occur at the maxima of the E_{tect}-curve, in our model they occur at the maxima of the E_{fault}-curve. The latter, arising from the slip heterogeneity along the fault, is not at all accounted for in the elastic rebound theory. Because present earthquake prediction models rely on the elastic rebound theory, the implications of this study for hazard assessment are evident.

References

[1] Ziv, A., and A. Cochard, Seismicity on a fault with depth-variable rate- and state- dependent friction: quasi-dynamic inherently-discrete model, in preparation.

[2] Reid, H. F., The mechanism of the earthquake, In *The California Earthquake of April 18, 1906, Report of the State Earthquake Investigation Commission,* Vol. 2, Washington, DC, Carnegie Institution, pp. 1–192, 1910.

[3] Schmittbuhl, J., J.-P. Villote, and S. Roux, A dissipation-based analysis of an earthquake fault model, *J. Geopys. Res.*, *101*, 27741–27764, 1996.

[4] Ben-Zion, Y., M. Eneva, and Y. Liu, Large earthquake cycles and intermittent criticality on heterogeneous faults due to evolving stress and seismicity, *J. Geopys. Res.*, *108*, 2307, doi:10.1029/2002JB002121, 2003.

[5] Rice, J. R., Spatio-temporal complexity of slip on a fault, *J. Geophys. Res.*, *98,* 9885-9907, 1993.

[6] Dieterich, J. H., Modeling of rock friction, 1. Experimental results and constitutive equations, *J. Geophys. Res.*, *84,* 2161–2168, 1979.

[7] Ruina, A., Slip instability and state variable friction laws, *J. Geopys. Res.*, *88,* 10359–10370, 1983.

[8] Ruina, A. L., Friction laws and instabilities: A quasistatic analysis of some dry frictional behavior, Ph.D. thesis, Brown Univ., Providence, R. I., 1980.

[9] Dieterich, J. H., Earthquake nucleation on faults with rate- and state- dependent strength, *Tectonophysics, 211,* 115–134, 1992.

[10] Ziv, A., and J. Schmittbuhl, The seismic cycle and the difference between foreshocks and aftershocks in a mechanical fault model, *Geophys. Res. Lett., 30(24)* 2237, doi:10.1029/2003GL018665, 2003.

[11] Ziv, A., and A. M. Rubin, Implications of rate-and-state friction for properties of aftershock sequence: quasi-static inherently discrete simulations, *J. Geopys. Res.*, *108*, 2051, doi:10.1029/2001JB001219, 2003.